



Isolation of coumarins with anti-*Trichophyton rubrum* activity from *Heracleum vicinum* Boiss.

Haishun Wu¹ · Mouyan Liu² · Shengdan Liu² · Huazhong Yu² · Huixin Chen³

Received: 15 November 2022 / Accepted: 25 April 2023 / Published online: 5 May 2023
© The Author(s) under exclusive licence to Sociedade Brasileira de Microbiologia 2023

Abstract

Heracleum vicinum Boiss., a perennial plant of Angelica in Umbelliferae, is mainly distributed in Sichuan and Hunan of China. *Trichophyton rubrum* is a common skin fungus causing dermatophyte. The previous experimental study found that the ethanol extract from *Heracleum vicinum* Boiss. had excellent anti-*Trichophyton rubrum* activity, especially the ethanol extract further extracted with petroleum ether and dichloromethane has the best antibacterial effect and has good potential for treating dermatophytes. In this study, *Heracleum vicinum* Boiss. was extracted with ethanol by microwave-assisted ultrasonic extraction method and isolated with silica gel column to obtain a coumarin compound M1-1 by the guidance of anti-*Trichophyton rubrum* activity, which was characterized by nuclear magnetic resonance spectroscopy (¹³C-NMR), hydrogen nuclear magnetic resonance (¹H-NMR), Fourier transform infrared spectroscopy (FTIR), high-resolution mass spectrometry (HR-ESI-MS), and ultraviolet (UV) and identified as imperatorin and belonged to coumarins, with the minimum inhibitory concentration (MIC) against *Trichophyton rubrum* of 12.5 µg/mL. According to the discussion on the inhibitory mechanism of the compound, we found that the compound may exert its inhibitory effect by destroying the mycelial membrane and inhibiting the mycelial growth of *Trichophyton rubrum*. In a word, imperatorin isolated from *Heracleum vicinum* Boiss. is expected to be used as an antibacterial agent to treat dermatophytes a potential natural compound against *Trichophyton rubrum*, and a template for drug development of dermatophytes the future.

Keywords *Heracleum vicinum* Boiss. · Imperatorin · Anti-*Trichophyton rubrum* · Antibacterial mechanism

Responsible Editor: Celia Maria de Almeida Soares

✉ Huazhong Yu
yuhuazhong.001@163.com

Haishun Wu
whs980116@163.com

Mouyan Liu
11953804324@163.com

Shengdan Liu
liushengdan22@163.com

Huixin Chen
chengchaoDG@163.com

¹ Key Laboratory of Hunan Forest Products and Chemical Industry Engineering, Jishou University, Zhangjiajie 427000, China

² College of Chemistry and Chemical Engineering, Jishou University, Jishou 416000, China

³ Guangdong Yutong Pharmaceutical Biotechnology Co., Ltd., Guangzhou 523000, China

Introduction

Dermatophytosis is the most common fungal infection in the world [1]. *Trichophyton rubrum* is the main fungus causing onychomycosis, tinea corporis, and other dermatomycoses [2, 3]. At present, the approved antifungal drugs mainly include terbinafine, itraconazole, fluconazole, and griseofulvin, but long-term use of these drugs usually causes many side effects such as hepatotoxicity [4, 5]. In recent years, plant natural compounds have been paid more and more attention by researchers and patients because of their wide biological and medical activities, safe use, and low cost [6–9].

At present, many studies showed the inhibition of *T. rubrum* by plant extracts and found many excellent plants and their effective components for inhibiting *T. rubrum*. For example, six Chinese medicine, such as *Scutellaria baicalensis* Georgi., *Coptis chinensis* Franch., *Phellodendron amurense* Rupr., *Rheum officinale* Baill., *Houttuynia cordata* Thunb, and *Stephania tetrandra* S. Moore, have inhibitory

effects on six drug-resistant bacteria, such as penicillin-resistant *Streptococcus pneumoniae*, methicillin-resistant *Staphylococcus aureus*, and *Escherichia coli* producing extended-spectrum β -lactamase, with their minimum inhibitory concentrations all below 0.031 g/mL [10] which has strong antibacterial activity. Ferrante [11] tested the inhibitory activity of five plant extracts (*Solidago decurrens* Lour., *Ononis spinosa*, *Peumus boldus*, *Epilobium angustifolium*, and *Phyllanthus niruri*) against *T. rubrum* and found that they were all effective, especially *Epilobium angustifolium* with the strongest inhibitory activity of which MIC against *T. rubrum* (CCF 4933) was 24.80 μ g/mL. Khalaf [12] found that ethanol extracts from the calyx leaves of *Hibiscus syriacus* Linn. had inhibitory effects on the growth of four skin fungi (*Trichophyton mentagrophytes*, *Trichophyton rubrum*, *Microsporum gypseum*, *Microsporum canis*) isolated from skin, hair, and nails. The results of Hutasoit [13] showed that the cocoa shell extract also had a good inhibitory effect on *T. rubrum*, with the diameter of the inhibition zone of its 96% ethanol crude extract could reach 37.22 mm. Goudjil [14] found that *Thymus capitatus* essential oil also has the effect of inhibiting *Trichophyton rubrum*. In all, there are more than 300 kinds of plant traditional Chinese medicines that have different degrees of antifungal effects up to 2020 [15]. The research for anti-dermatophyte, active components and antibacterial mechanism of natural plant compounds has gradually become a hot spot [16].

Heracleum vicinum Boiss., belonging to Umbelliferae, is a perennial herb with flowering and aromatic smell, widely distributed and complex in taxonomy [17], of which root is generally used as traditional Chinese medicine, having the effect of treating headache. As few studies on its stems and leaves, the plants of the same genus are similar in composition, but also distinct [18]. This genus mainly contains several natural chemical components such as volatile components (aliphatic esters, carbonyl groups, phenylpropene, and terpenes), non-volatile components (flavonoids, furanocoumarins, tannins, and alkaloids), and minerals. With the development of research, more new components have been found, such as a new compound trans-Cinnamic acid glycoside isolated by Wang from the root of *Heracleum dissectum* [19] and a new coumarin compound-9, 10-dihydro-10-hydroxy-9-methoxy-bergapten [20] by Zhang from the root of *Heracleum dissectum*.

This genus has a wide range of biological and pharmacological activities, such as anti-inflammatory, antibacterial, anticholinesterase, antioxidant, antiviral, cytotoxic, and anticancer activities [21–25]. *Heracleum persicum* has been shown to relieve flatulence and stomach pain [26] and protect kidney structure and function from gentamicin-induced damage [27]. The essential oil of *Heracleum rawianum* has antibacterial activity against various bacterial and fungal strains including *Escherichia coli*, *Pseudomonas*

aeruginosa, *Pseudomonas faecalis*, *Bacillus cereus*, *Staphylococcus aureus*, and *Candida albicans* and is more sensitive to fungal samples (*Candida albicans*) than bacteria, based on Hasheminya's [28] study on its antibacterial and antifungal activities. The alcohol extract of *Heracleum dissectum* Ledeb can effectively reduce body weight and improve blood lipid status, with antioxidant, anti-inflammatory and anti-insulin resistance effects by up-regulating adiponectin/AMP activated protein kinase signal transduction, as a candidate raw material for multi-target functional food with new molecular mechanism, as Son [29] said.

Although *Heracleum vicinum* Boiss. has important medical significance, there are few studies on its chemical constituents and antifungal activities. Therefore, it is of great significance to study the mechanism of inhibitory activity against skin fungi of the *Heracleum vicinum* Boiss. through isolated inhibitory compounds to further its understanding and development.

Materials

Heracleum vicinum Boiss. leaves were collected in Zhangjiajie, Hunan, China (110°53'E, 29°19'N) in October 2021; *T. rubrum* was purchased from Beina Biological Co., Ltd. (China); anhydrous ethanol, petroleum ether (boiling range: 60–90°C), ethyl acetate, dichloromethane, and other reagents and solvents are all analytical purity (directly used without further purification). The aqueous solution was prepared with deionized water (DI) from Milli-Q-Water (HEAL FORCE, China).

Experimental

Extraction and isolation

Weighing 1 kg of the powder of the leaves of *Heracleum vicinum* Boiss. under the conditions of ethanol concentration of 25%, solid-liquid ratio of 1:15, ultrasonic power of 220 W, extraction temperature of 80°C, and extraction time of 30 min (the extraction conditions optimized by the previous experimental study), microwave ultrasonic-assisted extraction (XH-300A computer microwave ultrasonic combined synthesis extractor-Beijing Xianghu Science and Technology Development Co., Ltd.), suction filtration, decompression and concentration, the ethanol extraction concentration of the leaves of *Heracleum vicinum* Boiss. were prepared. The extract was successively extracted with petroleum ether (boiling range: 60–90°C), dichloromethane, ethyl acetate, and n-butanol. The extract was concentrated under reduced pressure and dried at 60°C in the oven to obtain the extracts

of each part, and the extracts were tested for anti-*Trichophyton rubrum* activity.

The petroleum ether fraction and dichloromethane fraction had the strongest anti-*Trichophyton rubrum* activity, so we further separated the two extraction parts.

Using adopt silica gel column chromatography (wet column loading, dry sample loading) to further separate, took petroleum ether extract 3.13644 g, fully dissolved with the proper amount of dichloromethane, stirred and mixed with silica gel (100–200 mesh) 15 g evenly, and put it on a rotary evaporator to dry the solvent, which was the treated sample M. Applied absorbent cotton and quartz sand at the bottom of the chromatographic column, took 200 g of chromatographic silica gel (chromatographic grade, 100–200 mesh) and put it in a beaker, added with 500 mL of petroleum ether, stirred with a glass rod, and slowly poured it into chromatographic column (flash chromatographic column with sand plate storage ball, outer diameter: 46 mm, inner diameter: 40 mm, 500 mL, effective length: 457 mm, nodal pore diameter: 2 mm, 24/40 excellent grade-TITAN/Titan) to press it hard. Sample M was uniformly added to the top of the column and eluted with petroleum ether:dichloromethane:ethyl acetate (1:1:0.2) as mobile phase at a flow rate of 5 mL/min, and one eluent was collected every 10 mL. Each one was detected by thin-layer chromatography (TLC). The agent was petroleum ether:dichloromethane:ethyl acetate (1:1:0.2). Eluents of components with the same RF value were combined, concentrated under reduced pressure to dryness, and stored by numbering.

Took 0.8582 g of dichloromethane extract, fully dissolved it with the proper amount of dichloromethane, stirred with 5 g weigh silica gel (chromatographic grade 100–200 mesh), until mixed evenly, and placed it on a rotary evaporator to dry the solvent. Silica gel column chromatography was used, with the same method as above. Petroleum ether:ethyl acetate:methanol (1:1:0.2) was used as mobile phase for elution, and one eluent was collected every 10 mL. Using TLC detection, the eluents of components with the same RF value were combined, concentrated to dryness under reduced pressure, and numbered for preservation.

The active components were screened, and the structure was identified by detection of the anti-*T. rubrum* activity.

The recrystallization conditions are as follows: the crude crystal was added with ethanol according to the solid-liquid ratio of 1:20, dissolved by heating at 60°C, and crystallized in a refrigerator at –4°C, and white needle-like crystal can be obtained after seven days, that is, M1-1.

Structural characterization

One-dimensional NMR spectra were measured by JEOL JNM-ECS400 (600 MHz) spectrometer (JEOL, Tokyo, Japan). The chemical shift (δ) was expressed as ppm and the coupling

constant (J) as HZ. Infrared spectra were measured on a Fourier Transform Infrared Spectrometer (NICOLET-IS10, Thermo Fisher, USA). High-resolution electrospray ionization mass spectrometry (HR-ESI-MS) was tested on the VG Autospec-3000 spectrometer (VG, Manchester, England). Silica gel for column chromatography (200 mesh; purchased from Qingdao Ocean Chemical Plant). GF254 TLC silica gel plate with high efficiency (purchased from Rushan Sun Desiccant Co., Ltd.) is used for thin layer detection.

Isolated compounds and standards were determined by AGILENT 1260 HPLC system (AGILENT, San Jose, CA, USA) with G1315D DAD detector. Kromasil C18 column (4.6 mm \times 250 mm, inner diameter 5 μ m) was used to analyze samples. The mobile phase was eluted equivalently with acetonitrile and 0.1% acetic acid solution at a volume ratio of 55:45. Column temperature 40°C, flow rate 1.00 mL/min, injection volume 20 μ L, and detection wavelength 300 NM. Sample analysis was repeated 3 times.

Activation of strain

The strain was inoculated in potato glucose agar (PDA) medium and cultured at 28°C for 7 days to activate the strain. The spores of the activated strain were washed with normal saline, and the concentration of spores was calculated by blood cell counting plate, with 5×10^8 CFU.

Anti-*Trichophyton rubrum* activity detection

The Oxford cup inhibition zone method was used to test the anti-*Trichophyton rubrum*. The sample to be tested was added to the Oxford cup to make it diffuse in the PDA plate. The growth of *T. rubrum* near the Oxford cup was inhibited to form a transparent zone, that is, the inhibition zone. By measuring the diameter of the inhibition zone, the antibacterial effect of the sample to be tested was determined.

The specific operation is as follows: 20 mL of culture medium was poured into each culture dish. After solidification, 10 μ L of *T. rubrum* suspension was inoculated onto the culture dish by coating method. An Oxford cup was placed in the middle of each culture dish, and 20 μ L of liquid column separation products was added to each Oxford cup. When cultured at 28 °C for 5 days, the diameter of the inhibition zone was measured by the cross method. In a test plate, a single Oxford cup was used for the test (lest placing multiple Oxford cups would cause the inhibition zone to cross and affect the test results). The blank control was 30% ethanol.

Minimal inhibitory concentrations (MICs)

Using a plate containing M1-1, the M1-1 was diluted to five concentrations of 0.0625, 0.125, 0.25, 0.5, and 1 mg/mL by

double dilution method. Absorb 1 mL of M1-1 with different concentrations with a pipette gun, to add into 19 mL PDA culture medium, and then 100 μ L of the prepared *Trichophyton rubrum* suspension was sucked by a pipette gun and added to the plate, so that the final concentrations of M1-1-containing plates were 50, 25, 12.5, 6.25, and 3.125 μ g/mL, respectively, and then uniformly spread with a coating stick, and cultured in an incubator at 28°C. The concentration of complete sterile growth within 3 days was taken as the minimum inhibitory concentration (MIC). Three parallel experiments.

Effect on hyphae morphology

One milliliter spore suspension and 3 mL PDB medium were added into two sterile 10-mL test tubes separately and placed in a shaking table at 120 rpm and cultured at 28°C for 3 days. The experimental group was added with 1 mL 12.5 μ g/mL liquid M1-1, while the control group was with 1 mL ethanol and continued to culture. Three parallel tubes were set in each group and observed directly on the third, seventh, and fourteenth days, respectively.

Effect on radial growth of hyphae

T. rubrum was inoculated on PDA solid medium with a coating stick and cultured in a biochemical incubator at 28°C for 7 days. Used a punch with a diameter of 7 mm to take the *Trichophyton rubrum* blocks in the plate where they grow evenly for later use.

The sterilized PDA solid culture medium was quantitatively measured in 19 mL, cooled to 45°C and added with 1 mL of different concentrations (2MIC, MIC, 1/2 MIC, 1/4 MIC, 1/8 MIC). The final concentrations of the plate were 25, 12.5, 6.25, 3.125, and 1.5625 μ g/mL. The blank group was not treated with a liquid solution, and three parallel experiments were performed.

The center of the M1-1-containing plate was punched with a 7 mm diameter puncher, and then the prepared *Trichophyton rubrum* blocks were inoculated at the punched place, incubated in a 28°C incubator for 7 days, and the radial growth of hyphae was observed every day, and the diameter was measured by vernier caliper cross method.

Colony radial growth (mm) = average colony diameter – 7.

Percentage of inhibiting mycelium radial growth (%) = (colony diameter of blank group – colony diameter of experimental group)/colony diameter of blank group \times 100%.

Scanning electron microscopy (SEM) analysis

Added 200 μ L *Trichophyton rubrum* suspension and 1 mL PDB culture medium into EP tube, added 200 μ L liquid M1-1 after culture at 28°C for 3 days, added 200 μ L absolute ethanol in the blank, continued to culture for 24 h, fixed the samples with 2.5% glutaraldehyde fixative solution after fresh sampling, put them overnight at 4°C, poured out 2.5% glutaraldehyde fixative solution, rinsed the samples with 0.1 M phosphoric acid buffer with pH 7.0 for three times, each time for 15 min. The sample was fixed with 1% osmium acid solution for 2 h. The osmium acid waste solution was removed, and the sample was rinsed with 0.1 M, pH 7.0 phosphoric acid buffer solution for three times, each time 15 min. Samples were dehydrated with gradient concentrations (30%, 50%, 70%, 80%, 90%, and 95%) of ethanol solution for 15min each and then treated with absolute ethanol twice for 20 min each time. Then treated with the mixture of ethanol and isoamyl acetate (V/V=1/1) for 30 min and then added with isoamyl acetate for 1 h. Critical point drying. Coating and observation. The treated samples were observed under the scanning electron microscope.

The model used for scanning electron microscope: SU8100+energy spectrum Oxford ULTIImmAX65, critical point QUOROM K850 + gold spray Hitachi MC1000.

Fig. 1 *T. rubrum*: On potato dextrose agar medium (a). Under a microscope (b)

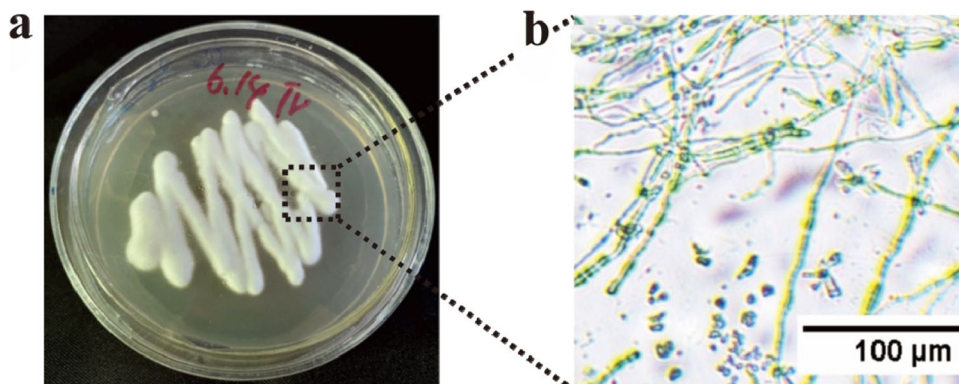
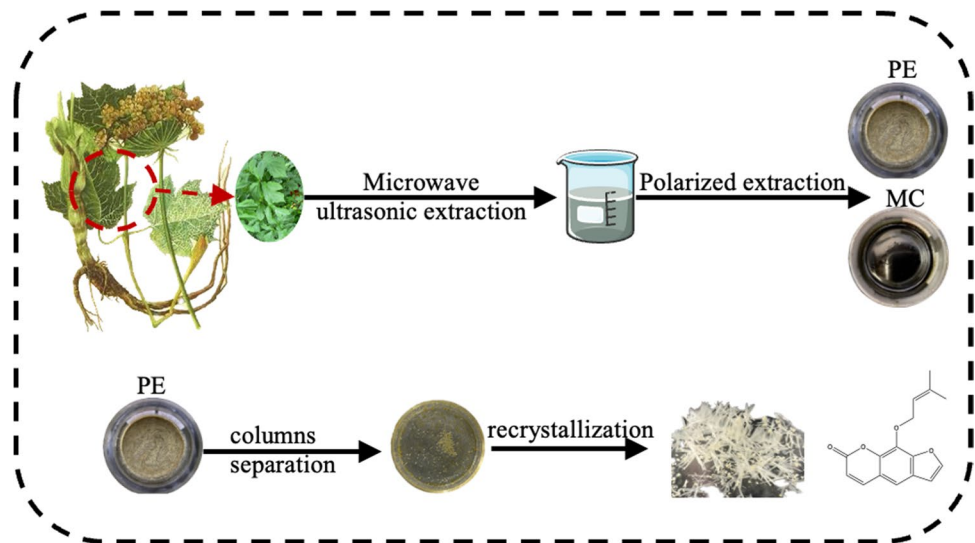


Fig. 2 Separation flow chart



Statistical analysis

Statistical analyses were carried out with the software GraphPad Prism 9. Each experiment was performed at least three. The data were subjected to Tukey's test for comparison of means at $P \leq 0.05$.

Results and discussion

The morphology of *Trichophyton rubrum* on potato dextrose agar media and under a microscope is shown in Fig. 1. The *Trichophyton rubrum* is a pathogenic fungus for humans and can cause skin fungal diseases such as tinea pedis, onychomycosis and tinea cruris. The pigmentation of *Trichophyton rubrum* is variable and strongly influenced by pH, ranging from white or yellow to wine red. Under alkaline conditions, *Trichophyton rubrum* has red pigmentation. While under acidic conditions, *Trichophyton rubrum* has yellow pigmentation [30]. Septate hyphae, small conidia are tear-drop-shaped, usually distributed along the hyphae and can be a large number, rare or missing, long, narrow, thin-walled, both sides of the wall parallel (pencil shape) [31].

State and activity of extracted components

The separation flow chart is shown in Fig. 2. Petroleum ether and dichloromethane were used to extract the concentrated solution of the microwave-assisted ultrasonic extraction of the leaves of *Heracleum vicinum* Boiss. PE is petroleum ether extract and MC is dichloromethane extract. The extract was separated by column, and the product M1 obtained by petroleum ether column separation was further recrystallized to obtain the active monomer M1-1.

After extracting 1 kg powder of *Heracleum vicinum* Boiss. with ethanol, the extract of 5.5584 g petroleum ether extract (khaki paste with a strong aroma) and 2.5054 g dichloromethane (brown, green oil paste with a strong aroma) were obtained.

In the extraction process, petroleum ether, dichloromethane, ethyl acetate, and n-butanol all had serious emulsification phenomena. Then, ultrasonic treatment for 30 min and high-speed centrifugation for 10 min at 8000 rpm can alleviate the emulsification phenomenon.

Oxford cup antibacterial test was carried out on silica gel column separation products, and the results showed that extracts had effects on *T. rubrum*. The antibacterial test of the silica gel column separation product was carried out by Oxford cup method. The antibacterial effect is shown in

Table 1 Anti-*Trichophyton rubrum* activity of silica gel column separation product

Species	Isolate	Petroleum ether extraction site	Isolate	Dichloromethane extraction site
		Bacteriostatic circle diameter (mm)		Bacteriostatic circle diameter (mm)
<i>T. rubrum</i>	M1	30.98	R1	33.73
	M2	26.37	R2	33.76
	M3	27.37	R3	8.12
	M4	28.93	R4	41.16
	M5	21.99	R5	25.47
	M6	15.22	R6	25.55
			R7	18.98
			R8	21.36
			R9	9.41
			R10	--

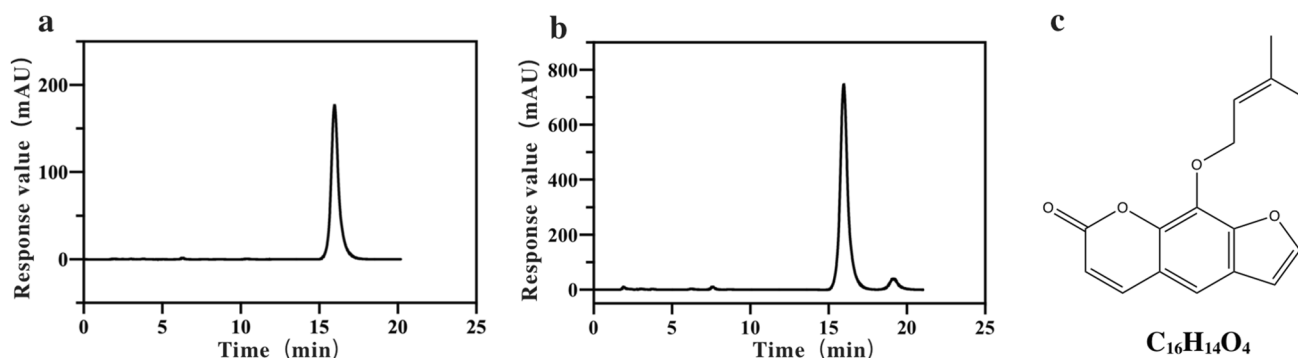


Fig. 3 Liquid chromatogram: imperatorin (a), M1-1 (b), imperatorin molecular formula (c)

Table 1, and the results show that it has an effect on *Trichophyton rubrum*.

Component M1-1 is a single component detected by thin layer chromatography. After concentration, a crystalline object is precipitated. M1-1 was further recrystallized and dried to obtain M1-1.

Figure 3 shows that the purity of M1-1 was 99% by high-performance liquid chromatography (HPLC), and the MIC was 12.5 $\mu\text{g}/\text{mL}$, as shown in Fig. 4

Compound M1-1 was obtained as a white needle crystal. In its mass spectrum, it showed a molecular ion peak at m/z 270.85 (calculated for $\text{C}_{16}\text{H}_{14}\text{O}_4$).

The ^1H NMR data for compound M1-1 are as follows: ^1H NMR (600 MHz, $\text{DMSO}-d_6$) δ 8.11–8.05 (m, 2H), 7.61 (s, 1H), 7.03 (d, $J = 2.2$ Hz, 1H), 6.37 (d, $J = 9.6$ Hz, 1H), 5.46 (tp, $J = 7.3, 1.5$ Hz, 1H), 4.86 (d, $J = 7.2$ Hz, 2H), 1.64 (d, $J = 1.6$ Hz, 3H), 1.59 (d, $J = 1.4$ Hz, 3H).

As shown in Fig. 5a, UV (MeOH) displayed maximum absorption bands at 217, 246 and 300 nm.

The FT-IR spectrum of compound M1-1 shows a characteristic band with strong intensity at around $1,720\text{ cm}^{-1}$, due to α, β -unsaturated-d-lactone. The bands at around 1586 and 1402 cm^{-1} are due to the presence of aromatic moiety and the bands at 1326 and 1295 cm^{-1} are because of

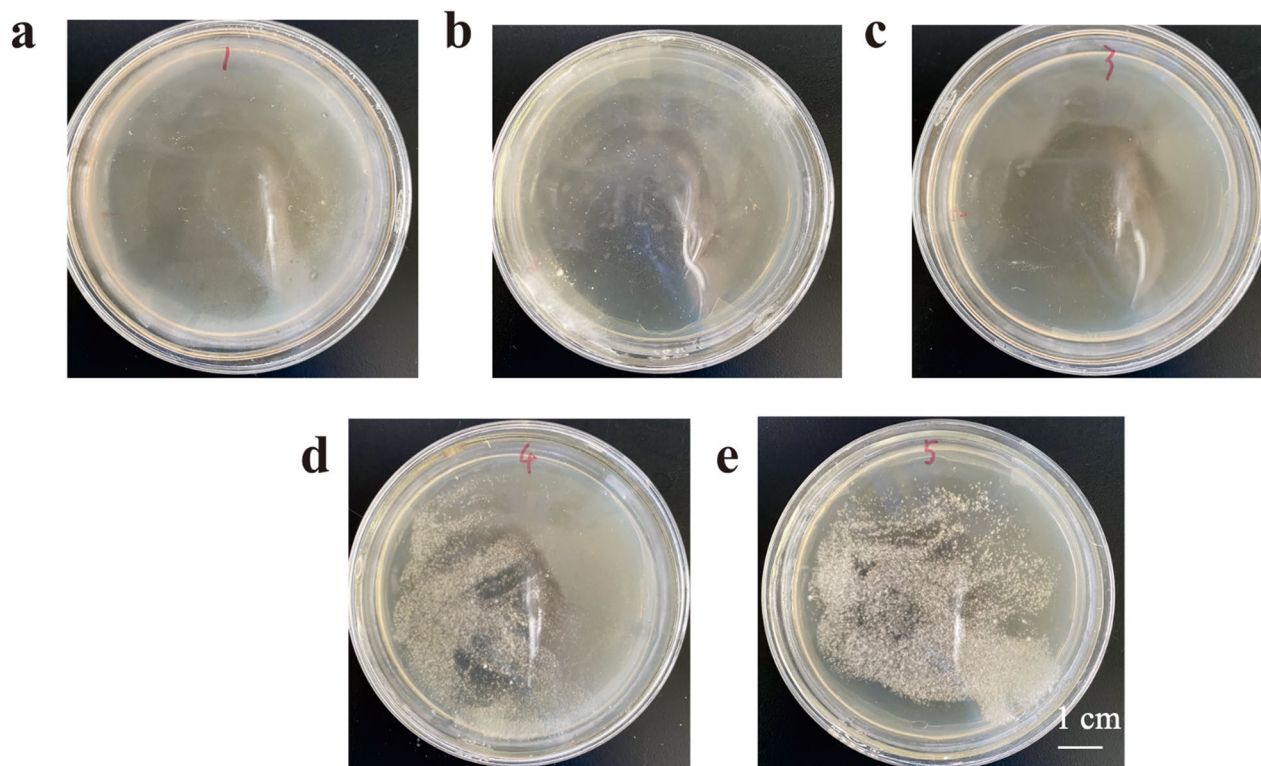


Fig. 4 MIC of M1-1 (a 50 $\mu\text{g}/\text{mL}$; b 25 $\mu\text{g}/\text{mL}$; c 12.5 $\mu\text{g}/\text{mL}$; d 6.25 $\mu\text{g}/\text{mL}$; e 3.125 $\mu\text{g}/\text{mL}$)

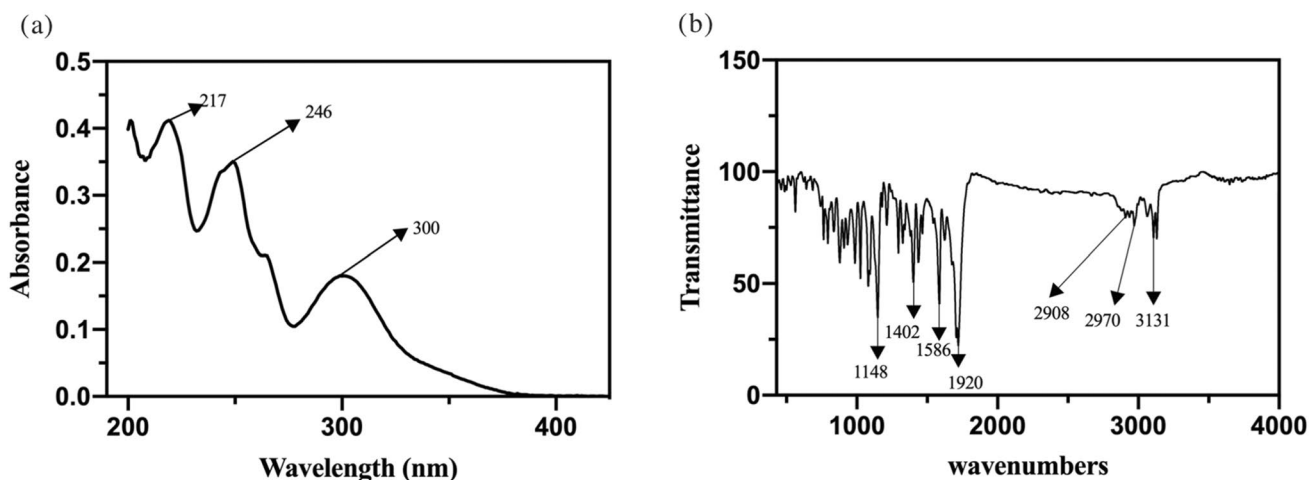


Fig. 5 UV (a), FTIR (b) of M1-1

gem-dimethyl. The asymmetric C–H stretching of methyl groups was observed at 2970 cm^{-1} and the symmetric one at around 2908 cm^{-1} . The compound displayed bands at 1465 and 1326 cm^{-1} due to the asymmetric and symmetric bending vibrations of methyl groups, respectively. The peak at 3131 cm^{-1} was assigned to aromatic C–H stretching. The compound displayed a peak at 1148 cm^{-1} , subsequently assigned to C–O stretching vibration.

Comparison of physical characteristics and spectral data of compound M1-1, with that reported in the literature [32, 33], confirmed it to be imperatorin.

Imperatorin is a furanocoumarin compound extracted from Umbelliferae plants, especially in *Angelicae dahuricae* Radix [34]. It has anti-inflammatory, analgesic, antibacterial, antiviral, anti-allergic, anti-tumor, reversing drug resistance of tumor cells, interacting with drug metabolic enzymes, and affecting cardiovascular and nervous systems.

It is one of the standard components of quality control in a variety of analgesic drugs [35]. In recent years, there have been more and more studies on imperatorin, such as modifying its structure and synthesizing its derivatives to increase its water solubility and increase its bioavailability. In addition to most of the pharmacological effects of coumarin, imperatorin may also treat osteoporosis, skin diseases, etc., and its mechanism of action has multi-channel and multi-target characteristics, but its target is not yet clear. At present, the activities of imperatorin reported in the literature mainly include the following: (1) inhibition of inflammatory response: imperatorin can inhibit the release of inflammatory mediators, such as interleukin- 1α , interleukin-6, and tumor necrosis factor- α . (2) Inhibition of free radicals: imperatorin can inhibit the formation of free radicals, thereby reducing cell damage. (3) Inhibition of apoptosis: imperatorin can inhibit apoptosis, thereby reducing

Fig. 6 Mycelium morphology of *T. rubrum*. Blank (a), M1-1 (b)

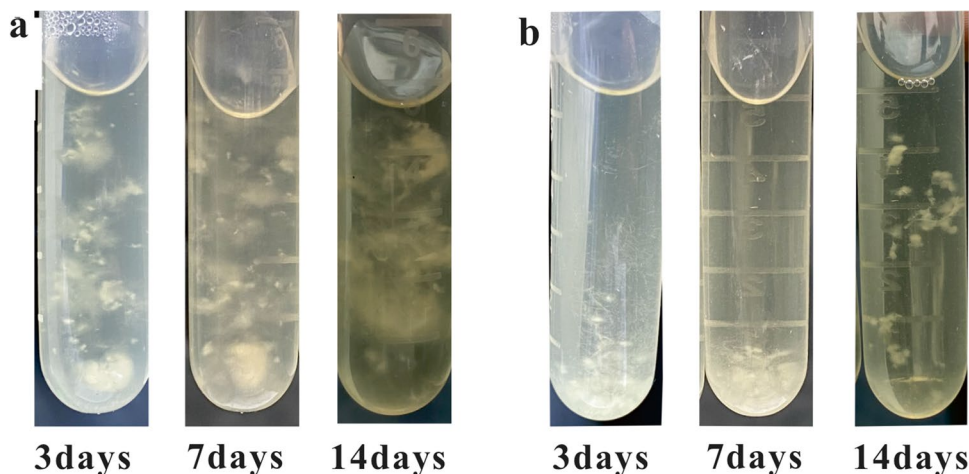
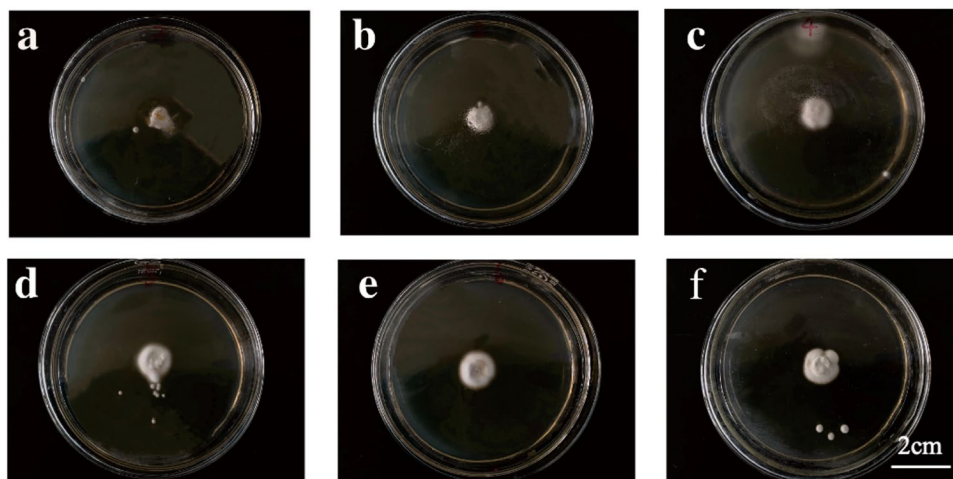


Fig. 7 Radial growth of *T. rubrum* mycelium (a 25 $\mu\text{g/mL}$; b 12.5 $\mu\text{g/mL}$; c 6.25 $\mu\text{g/mL}$; d 3.125 $\mu\text{g/mL}$; e 1.5625 $\mu\text{g/mL}$; f blank)



cell damage. (4) Inhibition of cell proliferation: imperatorin can inhibit cell proliferation, thereby reducing cell damage. (5) Inhibition of cell signal transduction: imperatorin can inhibit cell signal transduction, thereby reducing cell damage. (6) Inhibition of membrane lipid peroxidation: Imperatorin can inhibit membrane lipid peroxidation, thereby reducing cell damage [36, 37].

Effect of M1-1 on hyphal morphology of *T. rubrum*

T. rubrum produces hyphae that can penetrate the innermost skin of the host to injure the host [38, 39]. Therefore, the inhibitory effect of M1-1 on the mycelial growth of *T. rubrum* was studied in order to explore its inhibitory mechanism.

As can be seen from Fig. 6, the mycelium of *T. rubrum* became needle-like and no longer grew after adding M1-1 solution and cultured for 3 days, while the mycelium in the control group grew rapidly. After 7 days, there was little difference between the growth of the M1-1 treatment group and the control group. On the fourteenth day, the mycelium in the control group became large flocculent and the culture solution was turbid, while the mycelium in the M1-1 treatment group became thin flake, with clear culture solution. M1 of MIC dose can directly prevent the mycelium growth of *T. rubrum*.

Table 2 Inhibition rate of different concentrations of M1-1 on mycelium radial growth

	A	B	C	D	E
M1-1 solution concentration ($\mu\text{g/mL}$)	25	12.5	6.25	3.125	1.5625
Inhibiting mycelial growth rate (%)	43.56	18.67	4.8	4.6	3.6

Effect of M1-1 on radial growth of *T. rubrum* hypha

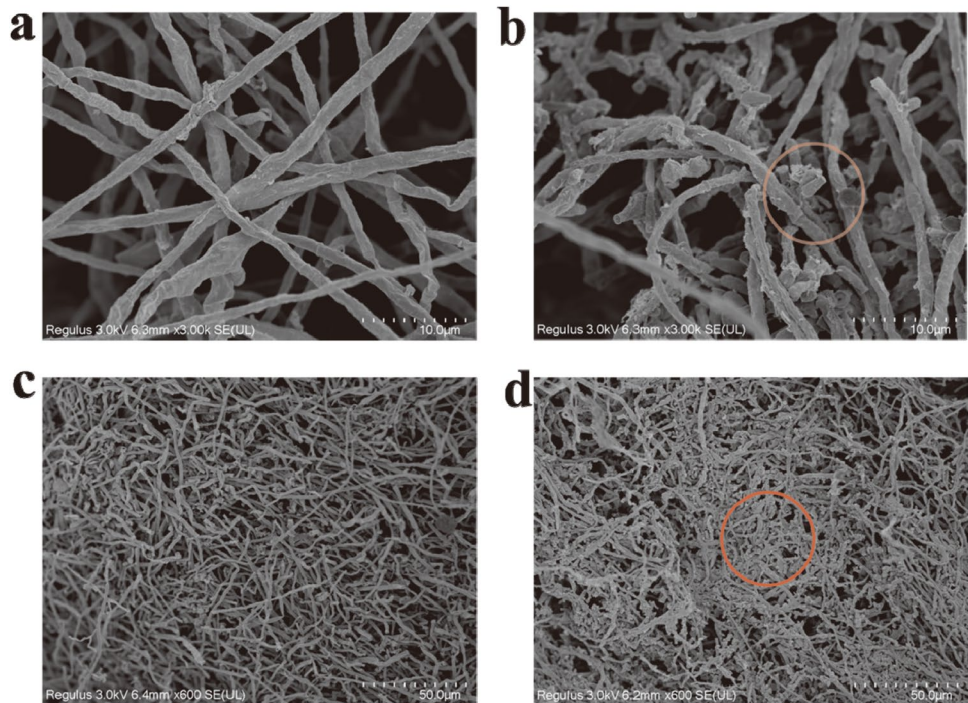
M1-1 can inhibit the radial growth of *T. rubrum* hyphae, as shown in Fig. 7 and Table 2, and the inhibition effect is proportional to the concentration of M1-1 liquid medicine. When the concentration of M1-1 was 1.5625 $\mu\text{g/mL}$, it began to inhibit the radial growth of *T. rubrum* mycelium, with the inhibition rate of 3.6%. When the concentration of M1-1 reached 25 $\mu\text{g/mL}$, the inhibition rate was 43.56%.

Scanning electron microscope

Figure 8 shows the scanning electron microscope of *T. rubrum* treated with M1-1 and without M1-1. The hyphae of *T. rubrum* treated with M1-1 alcohol solution are seriously broken, as shown in Fig. 8b, d. M1-1 inhibited and destroyed the mycelial growth and structure of *T. rubrum* to some extent. The hyphae were broken in many places, with peeled and mushy surfaces and overflowed contents. The hyphae underwent morphological changes such as contraction, flattening, bending, and twisting. These changes were similar to the antibacterial mechanism of magnoflorin against *T. rubrum* [4].

The main mechanism of antifungal compounds is to inhibit the synthesis of fungal nucleic acid and protein by destroying the integrity of the cell wall and cell biofilm and its biosynthesis [40]. The fungal cell wall is a dynamic structure that protects protoplasts from external osmotic impact, while ergosterol, as a unique lipid on the fungal cell membrane and an important structural component of the fungal cell membrane, stabilizes membrane structure and regulates the fluidity of fungal cell membrane by binding with phospholipids, playing an important role in ensuring the integrity of membrane structure, affecting the activity of membrane-binding enzymes, cell passability, and material transport [41, 42]. It is speculated that the mycelial structure of *T. rubrum* was destroyed by M1-1, resulting in a large number of ruptures and cell contents being lost in the fungus.

Fig. 8 SEM micrographs of *T. rubrum*: blank (a) (c), M1-1 (b) (d)



Conclusion

This report describes imperatorin, a coumarin compound isolated from the alcohol extract of *Heracleum vicinum* Boiss. and its inhibitory activity against *T. rubrum*, an important dermatophyte. After extraction, column chromatography separation, and crystallization, a high-purity monomer compound with the highest content of petroleum ether extract part and the best anti-*T. rubrum* activity was obtained (the purity was 99% by liquid chromatography, and the structure was identified as imperatorin). The coumarin has good antifungal activity against *T. rubrum*, with MIC of 12.5 µg/mL, of which the mechanism was preliminarily explored, providing a new idea for developing antifungal agents based on coumarin skeleton.

Acknowledgements The authors would like to thank Prof. Yu for the orientation and support to conduct of this work and Huixin Chen's support for experimental materials and funds.

Author contribution Each author has contributed significantly to this work. Haishun Wu designed and performed the experiments, analyzed the data, and edited the manuscript. Mouyan Liu and Shengdan Liu supervised the experiments, and Huazhong Yu wrote the manuscript. Huixin Chen provided experimental materials. All authors have reviewed, discussed, edited, and approved the final manuscript.

Declarations

Ethics approval Not applicable

Consent to participate Not applicable

Conflict of interest The authors declare no competing interests.

References

1. Khurana A, Sardana K, Chowdhary A (2019) Antifungal resistance in dermatophytes: recent trends and therapeutic implications. *Fungal Genet Biol* 132:103255. <https://doi.org/10.1016/j.fgb.2019.103255>
2. Lipner SR, Scher RK (2019) Onychomycosis clinical overview and diagnosis. *J Am Acad Dermatol* 80(4):835–851. <https://doi.org/10.1016/j.jaad.2018.03.062>
3. Zhan P, Liu W (2017) The changing face of dermatophytic infections worldwide. *Mycopathologia* 182(1-2):77–86. <https://doi.org/10.1007/s11046-016-0082-8>
4. Luo N, Jin L, Yang C et al (2021) Antifungal activity and potential mechanism of magnoflorine against *Trichophyton rubrum*. *J Antibiot* 74(3):206–214. <https://doi.org/10.1038/s41429-020-00380-4>
5. Eichhorn K, Uhrlass S, Nenoff P (2021) Chronisch rezidivierende tinea corporis durch ein terbinafin-resistentes isolat von *Trichophyton rubrum* - erfolgreiche therapie mit itraconazol. *J Dtsch Dermatol Ges* 19:27–30. <https://doi.org/10.1111/ddg.14470>
6. Taha M, Tartor YH, Abdul-Haq SIM et al (2022) Characterization and antidermatophyte activity of Henna extracts: a promising therapy for humans and animals dermatophytoses. *Curr Microbiol* 79(2):59. <https://doi.org/10.1007/s00284-021-02686-4>
7. Abu El-Wafa WM, Ahmed RH, MAH R (2020) Synergistic effects of pomegranate and rosemary extracts in combination with antibiotics against antibiotic resistance and biofilm formation of *Pseudomonas aeruginosa*. *Braz J Microbiol* 51(3):1079–1092. <https://doi.org/10.1007/s42770-020-00284-3>
8. Dsouza D, Nanjiah L (2018) Antibacterial activity of 3,3',4'-trihydroxyflavone from *Justicia wynaadensis* against diabetic wound and urinary tract infection. *Braz J Microbiol* 49(1):152–161. <https://doi.org/10.1016/j.bjm.2017.05.002>
9. Jesus RS, Piana M, Freitas RB et al (2018) In vitro antimicrobial and antimycobacterial activity and HPLC-DAD screening of phenolics from *Chenopodium ambrosioides* L. *Braz J Microbiol* 49(2):296–302. <https://doi.org/10.1016/j.bjm.2017.02.012>

10. Xu H, Yanle L, Zixing B et al (2019) Modern journal of integrated traditional Chinese and western medicine. *Modern J Integr Trad Chin Western Med* 28(32):3633–3637. <https://doi.org/10.3969/j.issn.1008-8849.2019.32.026>
11. Ferrante C, Chiavaroli A, Angelini P et al (2020) Phenolic content and antimicrobial and anti-inflammatory effects of *Solidago virgaurea*, *Phyllanthus niruri*, *Epilobium angustifolium*, *Peumus boldus*, and *Ononis spinosa* extracts. *Antibiotics-Basel* 9(11). <https://doi.org/10.3390/antibiotics9110783>
12. Khalaf A A, Jabar A, Sarab A A et al (2020) Activity evaluation of ginger alcoholic extract against *Candida albicans*
13. Hutasoit CMD, Setyaningsih Y, Pramono A (2020) Antifungal effectiveness of cacao bean shells extract (*Theobroma cocoa L.*) on *Trichophyton rubrum* growth in vitro. *Biomedika* 12(2):65–71. <https://doi.org/10.23917/biomedika.v12i2.10176>
14. Goudjil MB, Zighmi S, Hamada D et al (2020) Biological activities of essential oils extracted from *Thymus capitatus* (Lamiaceae). *S Afr J Bot* 128:274–282. <https://doi.org/10.1016/j.sajb.2019.11.020>
15. Ruqi H, Shuang W (2020) Research progress on anti-dermatophyte effect of Chinese medicine. *Chin J Cont End Dis* 35(4):432–434
16. Shakib P, Ali ASM, Javanmard E et al (2021) Anti-trichophyton effects of curcumin: a systematic review. *Anti-Infe Agents* 19(4). <https://doi.org/10.2174/2211352519666210202085849>
17. Yu Y, Downie SR, He X et al (2011) Phylogeny and biogeography of Chinese *Heracleum* (Apiaceae tribe Tordylieae) with comments on their fruit morphology. *Plant Syst Evol* 296(3–4):179–203. <https://doi.org/10.1007/s00606-011-0486-3>
18. Usjak L, Drobac M, Niketic M et al (2022) Chemical composition and chemosystematic evaluation of the fruit and root headspace fractions of selected *Heracleum* taxa from Southeastern Europe. *Bot Serb* 46(1):93–103. <https://doi.org/10.2298/botserb2201093u>
19. Wang Z-G, Mi J, Wang X-R et al (2018) A new cinnamic acid glycoside from roots of *Heracleum dissectum*. *Nat Prod Res* 32(2):133–140. <https://doi.org/10.1080/14786419.2017.1340285>
20. Zhang C, Deng S, Chen L et al (2022) A new coumarin isolated from the roots of *Heracleum dissectum Ledeb.* *Nat Prod Res* 36(13):3241–3246. <https://doi.org/10.1080/14786419.2020.1810033>
21. Majidi Z, Lamardi SNS (2018) Phytochemistry and biological activities of *Heracleum persicum*: a review. *J Integr Med-Jim* 16(4):223–235. <https://doi.org/10.1016/j.joim.2018.05.004>
22. Bahadori MB, Dinparast L, Zengin G (2016) The genus *Heracleum*: a comprehensive review on its phytochemistry, pharmacology, and ethnobotanical values as a useful herb. *Compr Rev Food Sci F* 15(6):1018–1039. <https://doi.org/10.1111/1541-4337.12222>
23. Ocal M, Altunoglu YC, Angeloni S et al (2022) Comparative content, biological and anticancer activities of *Heracleum humile* extracts obtained by ultrasound-assisted extraction method. *Chem Biodivers* 19(7). <https://doi.org/10.1002/cbdv.202101040>
24. Ozek G, Yur S, Goger F et al (2019) Furanocoumarin content, antioxidant activity, and inhibitory potential of *Heracleum verticillatum*, *Heracleum sibiricum*, *Heracleum angustisectum*, and *Heracleum ternatum* extracts against enzymes involved in Alzheimer's disease and type II diabetes. *Chem Biodivers* 16(4). <https://doi.org/10.1002/cbdv.201800672>
25. Taniguchi M, Yokota O, Shibano M et al (2005) Four coumarins from *Heracleum yunnanense*. *Chem Pharm Bull* 53(6):701–704. <https://doi.org/10.1248/cpb.53.701>
26. Behzadifar F, Marandi SJ, Majd A et al (2021) Genetic diversity analysis of the medicinal plant *Heracleum persicum Desfex Fischer*. *Genetika-Belgrade* 53(2):757–768. <https://doi.org/10.2298/genstr2102757b>
27. Akbaribazm M, Goodarzi N, Rahimi M et al (2021) Anti-inflammatory, anti-oxidative and anti-apoptotic effects of *Heracleum persicum L.* extract on rats with gentamicin-induced nephrotoxicity. *Asian Pac J Trop Bio* 11(2):47–58. <https://doi.org/10.4103/2221-1691.298628>
28. Hasheminya S-M, Dehghannya J (2021) Chemical composition, antioxidant, antibacterial, and antifungal properties of essential oil from wild *Heracleum rawianum*. *Biocatal Agric Biotechnol* 31:101913–101919. <https://doi.org/10.1016/j.bcab.2021.101913>
29. Son Y-J, Jung DS, Shin JM et al (2021) *Heracleum dissectum* Ledeb. ethanol extract attenuates metabolic syndrome symptoms in high-fat diet-induced obese mice by activating adiponectin/AMPK signaling. *J Funct Foods* 84. <https://doi.org/10.1016/j.jff.2021.104581>
30. Bleichert O, Zheng H, Zang X et al (2019) Influence of the cultivation medium and pH on the pigmentation of *Trichophyton rubrum*. *Plos One* 14(9). <https://doi.org/10.1371/journal.pone.0222333>
31. DAVIS L (2016) Guideline for the identification of important medical fungi, 5th edn China Medical Electronic Audio-visual Press
32. Koziol E, Skalicka-Wozniak K (2016) Imperatorin-pharmacological meaning and analytical clues: profound investigation. *Phytochem Rev* 15(4):627–649. <https://doi.org/10.1007/s11101-016-9456-2>
33. Banday JA, Mir FA, Qurishi MA et al (2013) Isolation, structural, spectral, and thermal studies of imperatorin micro-crystals from *Prangos pabularia*. *J Therm Anal Calorim* 112(3):1165–1170. <https://doi.org/10.1007/s10973-012-2683-x>
34. Fajinmi OO, Kulkarni MG, Benicka S et al (2019) Antifungal activity of the volatiles of *Agathosma betulina* and *Coleonema album* commercial essential oil and their effect on the morphology of fungal strains *Trichophyton rubrum* and *T. mentagrophytes*. *S Afr J Bot* 122:492–497. <https://doi.org/10.1016/j.sajb.2018.03.003>
35. Li XQ, Tan YQ, Li HJ, Lifeng Z, Feng S (2020) Research progress on pharmacological effects and mechanism of imperatorin. *Chin J Exp Trad Med Form* 26(18). <https://doi.org/10.13422/j.cnki.syfx.20201336>
36. Wu GY, Chen JY, Xu XL et al (2017) Research progress on the source and pharmacological effects of imperatorin. *23(20):54–56*. <https://doi.org/10.13862/j.cnki.cn43-1446/r.2017.20.018>
37. Koziol E, Skalicka-Wozniak K (2016) Imperatorin-pharmacological meaning and analytical clues: profound investigation. *Phytochemistry Reviews* 15(4):627–649. <https://doi.org/10.1007/s11101-016-9456-2>
38. Deng M, Xie L, Zhong L et al (2020) Imperatorin: a review of its pharmacology, toxicity and pharmacokinetics. *Eur J Pharmacol* 879. <https://doi.org/10.1016/j.ejphar.2020.173124>
39. Brand A (2012) Hyphal growth in human fungal pathogens and its role in virulence. *Int J Microbiol* 2012:517529. <https://doi.org/10.1155/2012/517529>
40. Balkis MM, Leidich SD, Mukherjee PK et al (2002) Mechanisms of fungal resistance - an overview. *Drugs* 62(7):1025–1040. <https://doi.org/10.2165/00003495-200262070-00004>
41. Avis TJ (2007) Antifungal compounds that target fungal membranes: applications in plant disease control. *Can J Plant Pathol* 29(4):323–329. <https://doi.org/10.1080/07060660709507478>
42. Nimrichter L, Rodrigues ML, Rodrigues EG et al (2005) The multitude of targets for the immune system and drug therapy in the fungal cell wall. *Microbes Infect* 7(4):789–798. <https://doi.org/10.1016/j.micinf.2005.03.002>

Publisher's note Springer Nature remains neutral with regard to jurisdictional claims in published maps and institutional affiliations.

Springer Nature or its licensor (e.g. a society or other partner) holds exclusive rights to this article under a publishing agreement with the author(s) or other rightsholder(s); author self-archiving of the accepted manuscript version of this article is solely governed by the terms of such publishing agreement and applicable law.